Available online at www.sciencedirect.com
SCIENCE DIRECT®
Journal of Molecular Catalysis A: Chemical 238 (2005) 35–40
JOURNAL OF MOLECULAR CATALYSIS A: CHEMICAL
www.elsevier.com/locate/molcata

Study of $La_{2-x}Sr_xCuO_4$ ($x = 0.0$, 0.5, 1.0) catalysts for NO + CO reaction from the measurements of O_2-TPD, H_2-TPR and cyclic voltammetry

Junjiang Zhu [a,b], Zhen Zhao [c], Dehai Xiao [a], Jing Li [a], Xiangguang Yang [a,*], Yue Wu [a]

[a] *Environmental Catalysis Group, Changchun Institute of Applied Chemistry, Chinese Academy of Sciences, Changchun 130022, China*
[b] *Graduate School of Chinese Academy of Sciences, Beijing 100039, PR China*
[c] *State Key Laboratory of Heavy Oil Processing, Beijing University of Petroleum, PR China*

Received 17 February 2005; received in revised form 16 March 2005; accepted 23 March 2005
Available online 13 June 2005

Abstract

Catalytic reduction of NO by CO was studied over perovskite-like $La_{2-x}Sr_xCuO_4$ ($x = 0.0$, 0.5, 1.0) catalysts prepared by citrate method and calcined at 900 °C. The catalysts were characterized by O_2-TPD, H_2-TPR and cyclic voltammetry (CV) measurements. Results obtained from CV were in well agreement with those obtained from O_2-TPD and H_2-TPR, suggesting that CV is also a powerful means in the study of heterogeneous catalytic reaction carried out at high temperatures. In O_2-TPD experiment, the desorption area of β oxygen, which was contributed by the oxygen adsorbed on the oxygen vacancy, increased with the increase of Sr content and was in the same order as the activity, indicating that the activity depended largely on the oxygen vacancy resulted by Sr addition. In H_2-TPR measurements, the increasing area of the first reduction peak indicating that the oxygen vacancy resulted by Sr addition plays important role in this peak, since the Cu^{3+} content in $La_{1.5}Sr_{0.5}CuO_4$ and $LaSrCuO_4$ is the same. And in the CV curves, the area of redox peak, which represents the amount of oxygen vacancy participating in the reaction, has close correlations with the activity of NO + CO reaction, while the symmetry of redox potentials does not contribute much to the activity. Overall, with the link of oxygen vacancy, CV was introduced and has obtained great success in explaining reaction in heterogeneous catalysis. Besides, from the result that none reductive peak was observed in the first CV curves of $LaSrCuO_4$, it suggested that the first step of a catalytic reaction is reduction, corresponding to the oxidation of catalyst i.e., $M^{n+}(Cu^{2+}) \rightarrow M^{(n+1)+}(Cu^{3+})$.

Keywords: NO + CO; $La_{2-x}Sr_xCuO_4$; Perovskite-like oxides; O_2-TPD; H_2-TPR; Cyclic voltammetry

1. Introduction

Compounds with formula A_2BO_4 generally have the tetragonal K_2NiF_4 structure when the radius of the A cation is $1.0 < r_A < 1.9$ Å, the radius of the B cation is $0.5 < r_B < 1.2$ Å. The larger A cation has nine-fold coordination and the smaller B cation has octahedral coordination. This structure can be described as containing alternate layering of perovskite (ABO_3) and rock-salt (AO) units with the nine coordinate A cation having a surrounding that is the average of what it would be in perovskite and rock salt [1]. These oxides (A_2BO_4), as well as perovskite (ABO_3), have a well-defined bulk structure and the composition of cations at both A and B sites can be variously changed without destroying the matrix structure, they therefore can be very useful as model systems to investigate the relationships between solid-state properties and catalytic performance of catalyst [2–4].

Various perovskite(-like) systems [5–9] have been investigated as catalysts for the reaction related with NO and CO (NO + CO), both of which are unwanted gas in the atmosphere. Voorhoeve et al. [5] have classified the NO + CO reaction on perovskites as an intrafacial process involving oxygen from the perovskite lattice. Pomonis and co-workers [8] have studied several kinetic models for NO + CO reaction and found that the oxygen mobility plays important role in the reaction. Dai et al. [9] investigated a various of catalysts and correlated the catalytic activity with the structural defect

* Corresponding author. Tel.: +86 431 5262228; fax: +86 431 5685653.
E-mail address: xgyang@ciac.jl.cn (X. Yang).

1381-1169/$ – see front matter © 2005 Elsevier B.V. All rights reserved.
doi:10.1016/j.molcata.2005.03.036

(mainly oxygen vacancies) and the redox (mainly transition metal ion couples) ability, and concluded that the generation of oxygen vacancies by A-site replacements favors the activation of O_2 and NO_x, while the modification of B-site ion oxidation states by aliovalent ion substitutions in A and/or B sites promotes the redox process of the catalyst, both of which favored the NO + CO reaction.

Previously, we have reported that cyclic voltammetry (CV) is a powerful means to investigate catalytic reactions in heterogeneous catalysis [10]. In this work, in addition to the CV measurement, we also performed the conventional O_2-TPD and H_2-TPR measurements to investigate the NO + CO reaction, since O_2-TPD measurement is known as an effective method to investigate reactivity on catalyst surface, while H_2-TPR measurement is widely used to characterize redox properties of the catalyst. The results obtained from CV were in well agreement with those obtained from O_2-TPD and H_2-TPR, indicating that CV measurement can be applied to investigate hetergeneous catalytic reaction occurred at high temperatures. The area of redox peak, which represents the amount of oxygen vacancy (i.e., "F center", $Cu^{2+}[\,] \rightarrow Cu^{3+}[e]$) participating in the reaction, has a close correlations with the activity of NO + CO reaction, due to the existence of the reducing agent (CO).

2. Experimental

The samples, $La_{2-x}Sr_xCuO_4$ ($x = 0.0$, 0.5, 1.0), were prepared by citrate combustion method as described elsewhere [11]. Briefly, to an aqueous solution of La^{3+}, Sr^{2+}, Cu^{2+} nitrates (all in AR. grade purity) with appropriate stoichiometry, a solution of citric acid 100% in excess of cations was added. The resulting solution was evaporated to dryness, and then the precursors were decomposed in air at 300 °C, calcined at 600 °C for 1 h, and finally pelletized and calcined at 900 °C in air for 6 h. The synthesized pellets were pulverized to ca. 40–80 mesh size to be used.

Powder X-ray diffraction (XRD) data were obtained from a X-ray diffractometer (type D/MAX-II B Rigaku) over the ranger $20^\circ < 2\theta < 80^\circ$ at room temperature, operating at 40 kV and 10 mA, using Cu Kα radiation combined with nickel filter.

Temperature programmed desorption of oxygen (O_2-TPD) was carried out in a conventional apparatus equipped with TCD [12,13]. The samples (0.25 g) were first treated at 850 °C for 1 h in oxygen and cooled to room temperature in the same atmosphere, then swept with helium at a rate of 35 mL/min until the base line on the recorder remained unchanged. Finally, the sample was heated at a rate of 35 °C/min in helium to record the TPD spectra.

Temperature programmed reduction of hydrogen (H_2-TPR) was carried out on the same apparatus as that in O_2-TPD. The samples (0.1 g) were first treated at 850 °C for 1 h in oxygen and cooled to room temperature in the same atmosphere, then swept with 8% H_2/N_2 at a rate of 35 mL/min until the base line on the recorder remained unchanged. Finally, the sample was heated at a rate of 20 °C/min in 8% H_2/N_2 to record the TPR spectra.

Cyclic voltammetry (CV) was measured in a conventional two-compartment, three-electrode cell as described in our previous work [10].

Steady-state activities of catalysts were evaluated using a single-pass flow micro-reactor made of quartz, with an internal diameter of 6 mm. The reactant gas (0.4% NO + 0.4% CO/He) was passed through 0.5 g catalysts at a rate of 22.5 mL/min. The gas composition was analyzed before and after the reaction by an online gas chromatography, using molecular sieve 5A column for separating NO, N_2 and Porapork Q for CO_2. Before the data were obtained, reactions were maintained for a period of ∼2 h at each temperature to ensure the steady-state conditions. The activity was evaluated as follows: NO conversion = $([NO]_{in} - [NO]_{out})/[NO]_{in}$, where $[NO]_{in}$ and $[NO]_{out}$ are the inlet and outlet concentration of NO, respectively.

3. Results and discussion

3.1. XRD study of samples

Fig. 1 showed the powder X-ray diffraction patterns of the samples (also see Table 1). All the samples are in single perovskite-like phase with A_2BO_4 structure. The structure of La_2CuO_4 is orthorhombic, while the structure of $La_{1.5}Sr_{0.5}CuO_4$ and $LaSrCuO_4$ is tetragonal. In this work, we represented the samples as $La_{2-x}Sr_xCuO_4$, although the actual composition is $La_{2-x}Sr_xCuO_{4\pm\lambda}$.

It is known that for perovskite-like oxides with A_2BO_4 structure, when A-site cations (i.e., La^{3+}) were substituted by low valence cations (i.e., Sr^{2+}), the average oxidation number of B-site cations (i.e., Cu^{2+}), as well as the content of oxygen vacancy will increase, in order to satisfy the principle of electroneutrality. The average oxidation number of B-site cations was chemically determined by iodometric titration [14] without treatment of the as-prepared samples. The stoichiometry was calculated on the assumption that the metals

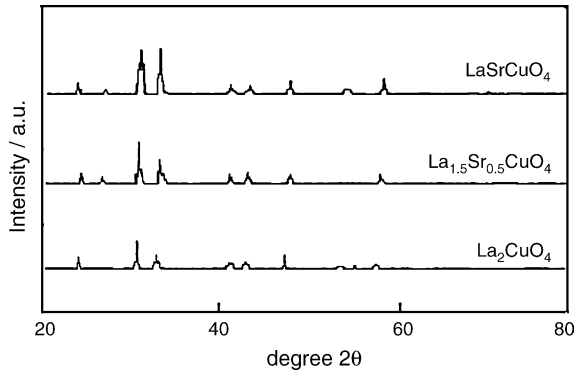

Fig. 1. X-ray diffraction patterns of $La_{2-x}Sr_xCuO_4$ ($x = 0.0$, 0.5, 1.0).

Table 1
The physical properties and catalytic activities at different temperatures of $La_{2-x}Sr_xCuO_{4+\lambda}$ ($x = 0.0, 0.5, 1.0$)

Catalysts	Structure	SSA[a] (m^2/g)	Oxidation no. of Cu[b]	λ[c]	NO conversion at different temperatures (°C)/%[d]								$S_{300-600\,°C}$
					250	300	350	400	450	500	550	600	
La_2CuO_4	Orthorhombic	2.5	2.02	+0.01	0	0	0	1.0	1.3	1.8	23.3	86.5	6.1
$La_{1.5}Sr_{0.5}CuO_4$	Tetragonal	2.4	2.24	−0.13	0	0	1.8	60	87.9	95.6	98.1	97.4	73.2
$LaSrCuO_4$	Tetragonal	2.6	2.24	−0.38	0	0	8.6	96.8	97.5	97.6	98.3	98.8	168

[a] Specific surface area.
[b] Average oxidation number of Cu.
[c] λ in $La_{2-x}Sr_xCuO_{4+\lambda}$ ($x = 0.0, 0.5, 1.0$).
[d] NO conversion in NO + CO reduction.

were present as either a mixture of Cu^{2+} and Cu^{3+} or Cu^{+} and Cu^{2+}, and other elements were present as La^{3+}, Sr^{2+} and O^{2-}, respectively. The results were listed in Table 1.

The amount of non-stoichiometry oxygen (λ) increased continuously with the substitution of Sr for La, due to the low valence of Sr^{2+} (comparing with that of La^{3+}); while for the average oxidation number of copper, it increased with the increase of Sr content (x) at the beginning ($0 \le x \le 0.5$), but kept constant (+2.24) at $x \ge 0.5$ no matter the amount of La is replaced by Sr. This suggested that the average oxidation number of copper in this system reached only +2.24, due to the instability of Cu^{3+} ions [15,16]. At $x \ge 0.5$, the decreasing charge caused by the excess substitution of Sr^{2+} for La^{3+} was compensated totally by increasing the amount of non-stoichiometry oxygen (λ), since the average oxidation number of copper cannot be elevated at $x > 0.5$. The oxidation number is formal, and it is possible that O^{-} is present instead of Cu^{3+} [17]. The surface composition, the oxidation number of copper and the non-stoichiometric oxygen (λ), which were estimated from X-ray photoelectron spectra (i.e., Cu $2p_{3/2}$ and O 1s) [12], were close to those of the catalysts listed in Table 1.

3.2. O_2-TPD

Fig. 2 showed the O_2-TPD profiles of the samples. In general, the desorption peaks plotted from the perovskite-like mixed oxides contain three kinds of oxygen species [18]. The desorption peak appeared at $T < 500\,°C$ is ascribed to the oxygen chemically adsorbed on the surface (denoted as: α oxygen); the desorption peak appeared at $500 < T < 800\,°C$ is ascribed to the oxygen chemically adsorbed on the oxygen vacancy (denoted as: β oxygen); and the desorption peak appeared at $T > 800\,°C$ is ascribed to the oxygen escaped from the lattice (denoted as: γ oxygen). One should note that in the samples of $La_{1.5}Sr_{0.5}CuO_4$ and $LaSrCuO_4$, there appeared a shoulder peak at the range of $500 < T < 800\,°C$, which might be attributed to the desorption of oxygen caused by the reciprocity of Cu^{3+} and O^{2-}, due to the instability of Cu^{3+} [15].

The peak maximum temperature (T_M) and the corresponding desorption area in O_2-TPD profile of each catalyst were calculated and listed in Table 2. No α oxygen desorption peak was observed in all the three samples. In the β oxygen desorption peaks, the desorption area of La_2CuO_4 was small due to the lack of Sr^{2+}, which implied that the oxygen vacancy produced was none or less; while large desorption areas were observed for $La_{1.5}Sr_{0.5}CuO_4$ and $LaSrCuO_4$, due to the Sr addition. The desorption area of β oxygen were in the same sequence as that of the non-stoichiometric oxygen (λ), suggesting that the desorption peaks appeared at this temperature range were contributed by the non-stoichiometric oxygen (λ). The desorption peak of γ oxygen depended on many factors. In addition to the structure and the oxygen deficiency, the oxidability of B-site cation also has large effect on the desorption of γ oxygen, especially under the condition that the structure was not destroyed [15]. Therefore, in the present case, the desorption area of γ oxygen depended mainly on the oxidability of B-site cation. The peak area desorbed at the range of 300–600 °C was calculated and listed in Table 2

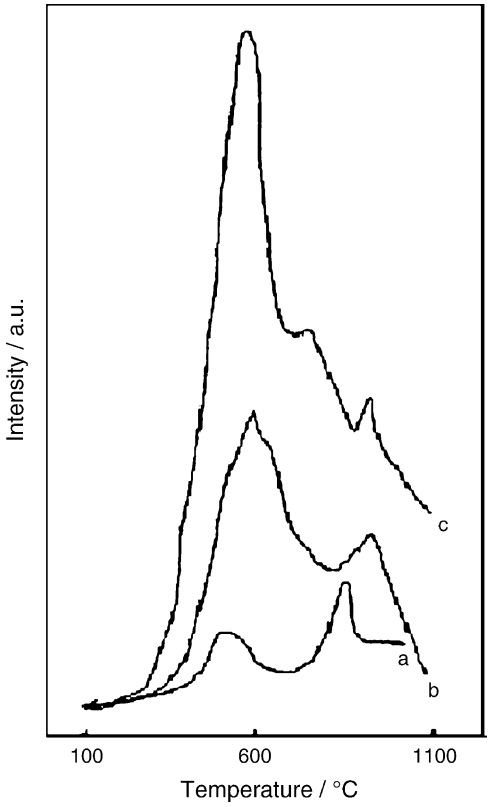

Fig. 2. O_2-TPD profiles obtained from $La_{2-x}Sr_xCuO_4$: (a) La_2CuO_4; (b) $La_{1.5}Sr_{0.5}CuO_4$; (c) $LaSrCuO_4$.

Table 2
Data measured and calculated in O_2-TPD and H_2-TPR measurements of $La_{2-x}Sr_xCuO_{4+\lambda}$ ($x = 0.0, 0.5, 1.0$)

Catalyst	Data obtained from O_2-TPD									Data obtained from H_2-TPR		
	α oxygen		β oxygen				γ oxygen		$S_{300-600\,°C}$	$Cu^{3+} \rightarrow Cu^{2+}$	$Cu^{2+} \rightarrow Cu_2O$	Cu^{3+} (%)
	T (°C)	S (cm^2)	T_1 (°C)	S (cm^2)	T_2 (°C)	S (cm^2)	T (°C)	S (cm^2)		T_1 (°C)	T_2 (°C)	
La_2CuO_4	–	–	501	6.1	–	–	875	8.2	6.1	–	698	2.0
$La_{1.5}Sr_{0.5}CuO_4$	–	–	570	73.2	755	20.1	948	11.3	73.2	453	592	24.0
$LaSrCuO_4$	–	–	576	168.0	721	67.2	918	44.8	168	450	601	24.0

also, in order to correlate the activity of the reaction, which was performed in the same temperature range. In this work, CO was totally oxidized at 600 °C over the three catalysts, and thus it (600 °C) was selected to be the upper temperature of the reaction.

3.3. H_2-TPR

In Fig. 3 the results of samples from H_2-TPR measurements were presented. In general, there are two kinds of reactant species participating in the reaction; one is the non-stoichiometric oxygen, including the excess oxygen and the oxygen adsorbed on the oxygen deficiency, the other is B-site cations with high oxidative state. For La_2CuO_4, in which no Sr was added, none oxygen vacancy and Cu^{3+} ion (only 2%) was formed and there has excess oxygen (see Table 1), the first reduction peak ($T = 503$ °C), then, was mainly ascribed to the reduction of excess oxygen, reaction (1):

$$La_2CuO_{4+x} + (x+y)H_2 \rightarrow La_2CuO_{4-y} + (x+y)H_2O \quad (1)$$

The fact that there still existed a large amount of La_2CuO_4 with orthorhombic structure in the sample after the first reduction peak (which were detected by XRD patterns, not shown here) certified that reaction (1) is the main reaction occurred at $T < 503$ °C. The second reduction peak thus was ascribed to the reduction of Cu^{2+} to Cu_2O, reaction (2):

$$2Cu^{2+} + H_2 + 2O^{2-} \rightarrow Cu_2O + H_2O \quad (2)$$

This was supported by the fact that the color of sample is red after the reduction at $T = 900$ °C. Certainly, some samples with red color were also observed after the first reduction peak ($T = 503$ °C), but the amount is little. That is to say, reaction (2) might occur at $T < 503$ °C but it is not the major reaction.

For $La_{1.5}Sr_{0.5}CuO_4$ and $LaSrCuO_4$, in which large amount of Sr were added, lots of oxygen vacancies were produced and some of Cu^{2+} ions were oxidized to Cu^{3+} ions. The first two split reduction peaks were mainly contributed by the Cu^{3+} ions and β oxygen (O^-), corresponding to reactions (3) and (4), respectively. (*Note:* the following equations were deduced from the XRD patterns after each reduction peak, and from the number of electrons transferred in the reaction. The number of electrons were calculated from the corresponding reduction peak area that were evaluated with CuO as the references, as suggested by Patcas et al. [19]. Here, the dealing procedure were not shown for simplification.)

$$2Cu^{3+} + O^{2-} + H_2 \rightarrow 2Cu^{2+} + H_2O \quad (3)$$

$$4O^- + 2Cu^{2+} + 3H_2 \rightarrow Cu_2O + 3H_2O \quad (4)$$

The second reduction peak was ascribed to the reduction of Cu^{2+} to Cu_2O, reaction (5):

$$2Cu^{2+} + H_2 + 2O^{2-} \rightarrow Cu_2O + H_2O \quad (5)$$

Table 2 also listed the peak maximum temperature (T'_M) of each reduction peak and the corresponding reduction species, which was confirmed by the XRD patterns after each reduction peak. For La_2CuO_4, the content of Cu^{3+} ions is little (2%) due to the lack of Sr, therefore, the first reduction peak was mainly contributed by the non-stoichiometric oxygen (λ). While for $La_{1.5}Sr_{0.5}CuO_4$ and $LaSrCuO_4$, the first reduction peak was contributed both by the higher oxidative state Cu^{3+} ions and by the non-stoichiometric oxygen (λ). The

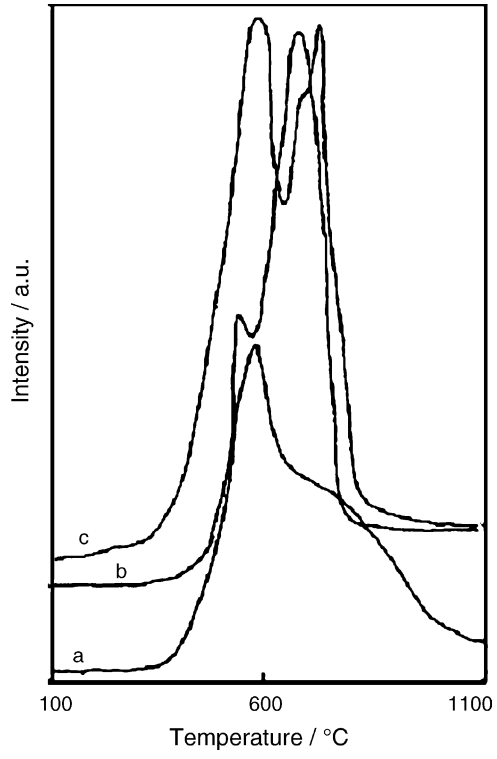

Fig. 3. H_2-TPR profiles obtained from $La_{2-x}Sr_xCuO_4$: (a) La_2CuO_4; (b) $La_{1.5}Sr_{0.5}CuO_4$; (c) $LaSrCuO_4$.

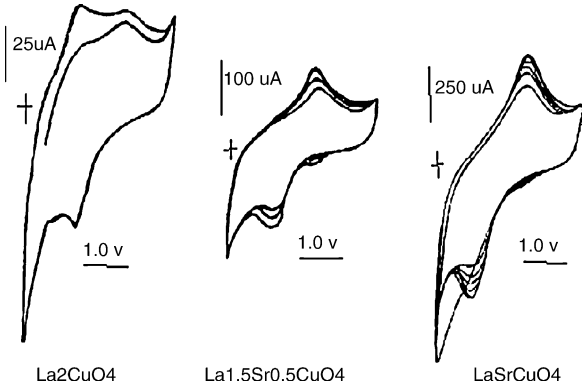

Fig. 4. Cyclic voltammetry curves of $La_{2-x}Sr_xCuO_4$ ($x = 0.0, 0.5, 1.0$).

large reduction peak area of $LaSrCuO_4$ is ascribed to the more amount of non-stoichiometric oxygen (λ) produced in it, since the Cu^{3+} content in the both catalysts is the same. The T'_M of $La_{1.5}Sr_{0.5}CuO_4$ and $LaSrCuO_4$ is similar but is lower than that of La_2CuO_4, suggesting that the Sr addition strengthen the oxidability of the catalyst. For the second reduction peak of La_2CuO_4, the peak area is smaller and the T'_M is higher than those of $La_{1.5}Sr_{0.5}CuO_4$ and $LaSrCuO_4$, suggesting that the Sr addition promotes the mobility of lattice oxygen or makes the structure unstable, which thus lowered the T'_M and enlarged the peak area.

3.4. Cyclic voltammetry

The cyclic voltammetry (CV) curves of the samples were shown in Fig. 4. For all the samples, the peak area of the oxidative potential was the same as that of the reductive potential, and the area of redox peaks, which represents the number of Cu ions participating in the reaction, i.e., "F center" ($Cu^{2+}[\,] \rightarrow Cu^{3+}[e]$), increased with the increase of Sr content, suggesting the increase of the number of oxygen vacancies. This is in accordance with the non-stoichiometry oxygen (λ) measured in them, i.e., $La_2CuO_4 < La_{1.5}Sr_{0.5}CuO_4 < LaSrCuO_4$. The reductive potential decreased with the increase of Sr content, indicating the enhancement of oxidability of samples. Besides, it should be noted that the first redox cycle of $LaSrCuO_4$ was irreversible; no reductive peak appeared in the first cycle, suggesting that the first step of catalytic reaction is reduction (corresponding to Cu^{2+} to Cu^{3+}), since the reduction of Cu^{3+} to Cu^{2+} cannot occur in the first cycle.

3.5. Catalytic activity

Catalytic activities of samples for NO + CO reduction at different temperatures were listed in Table 1. The activity increased with the increase of reaction temperature and depended largely on the catalysts. For La_2CuO_4 without Sr addition, the activity is low (<25%) until 600 °C, while for $La_{1.5}Sr_{0.5}CuO_4$ and $LaSrCuO_4$, high activity was gained even at 400 °C (reached 60 and 96.8%, respectively), indicating that the Sr addition facilitates NO + CO reaction to occur. The reason might be that the Sr addition induced the formation of oxygen vacancy, which is an important part of the active site of the reaction. Besides, by correlating the activity with the oxygen desorption area $S_{300–600\,^\circ C}$ contributed by the β oxygen (see O_2-TPD), it was found that the activity was in the same sequence as the oxygen desorption area $S_{300–600\,^\circ C}$, suggesting that the oxygen vacancy (β oxygen) do favor the NO + CO reaction.

It is generally accepted that the first step of the reaction is NO adsorption and dissociation on the active site [20,21], described as reactions (6) and (7):

$$M^{3+}–[\,]–M^{2+} + NO = M^{3+}–[NO^-]–M^{3+} \quad (6)$$

$$2M^{3+}–[NO^-]–M^{3+} = 2M^{3+}–[O^-]–M^{3+} + N_2 \quad (7)$$

$$M^{3+}–[O^-]–M^{3+} + CO = M^{3+}–[\,]–M^{2+} + CO_2 \quad (8)$$

where M represents Cu; "[ ]" represents the oxygen vacancy. After NO adsorption and dissociation, the oxygen left on the oxygen vacancy can be removed easily through the reaction (8) due to the existence of reducing agent (CO) and thus, the NO adsorption and dissociation steps became rate limiting. The more the amount of oxygen vacancies is, the more the amount of NO being adsorbed. As a result, the activity depends largely on the oxygen desorption area ($S_{300–600\,^\circ C}$) and the highest activity was obtained on $LaSrCuO_4$, which possessed the most amount of oxygen vacancy.

Results obtained from CV measurements supported the above conclusions. It has been noted above that no reductive peak appeared in the first CV curves of $LaSrCuO_4$, which certifies that the first step of the reaction is NO adsorption, corresponding to $Cu^{2+} \rightarrow Cu^{3+}$. For $LaSrCuO_4$, the redox peak area is in the largest while the symmetry of the redox potentials is the poorest. The redox peak area means the amount of oxygen vacancy (i.e., "F center", see above) participating in the reaction, while the symmetry of redox potentials is a measure of the transformation of transition metal, i.e., $M^{n+} \Leftrightarrow M^{n+1}$. The more the symmetry of redox potentials, the easier the transformation of $M^{n+} \Leftrightarrow M^{n+1}$, and the quicker the catalytic cycle running on the catalyst. However, in NO + CO reduction reaction, because of the existence of reducing agent (CO), the redox potentials of catalyst will be largely modulated according to the Nerst equation: $\Delta E = -(RT/nF)\ln([\text{oxidizer}]/[\text{reducer}])$, resulting in the reduction of oxidative potential and the raise of reductive potential and finally making them become symmetry [10]. Namely, ΔE of catalyst is not an intrinsic factor in deciding the catalytic activity of NO + CO reduction reaction due to the existence of reducing agent. The reversible active sites or the redox peak area in CV curves of catalyst, then, became the crucial factor in determining the activity of NO reduction. The larger the redox area is, the more the amount of oxygen vacancy participating in the reaction will be and thus, more amount of NO being adsorbed and disso-

ciated. As a result, the activity increased with the increase of the non-stoichiometry oxygen (λ) and $LaSrCuO_4$ showed the highest activity.

In all, it can be concluded that the redox peak area, which represents the amount of oxygen vacancy participating in the reaction, has close correlations with the activity of NO + CO reduction, whereas the symmetry of redox potentials does not relate much to the activity due to the existence of reducing agent. This is in accordance with the results obtained from O_2-TPD and H_2-TPR, indicating that the properties of CV curves also have close correlations with the activity of heterogeneous catalytic reaction occurred at high temperatures range.

4. Conclusions

Perovskite-like mixed oxides ($La_{2-x}Sr_xCuO_4$, $x = 0.0, 0.5, 1.0$) used as catalysts for NO + CO reaction were studied and characterized by O_2-TPD, H_2-TPR and CV measurements, all of which supported that the amount of oxygen vacancy (represented by the area of redox peak in CV curves) resulted by the Sr addition has close correlations with the activity of NO + CO reduction and hence, $LaSrCuO_4$ showed the highest activity for the reaction. While the symmetry of redox potentials does not relate much to the activity of NO + CO reduction due to the existence of reducing agent, which can modulate the ΔE value through the Nerst equation. The irreversible redox peak (no reductive peak was observed) in the first CV curves of $LaSrCuO_4$ suggests that the first step of the reaction is reduction, corresponding to the oxidation of catalyst, i.e., $M^{n+}(Cu^{2+}) \rightarrow M^{(n+1)+}(Cu^{3+})$. The so accordant results obtained from O_2-TPD, H_2-TPR and CV measurements suggested that CV is indeed a powerful means for the study of heterogeneous catalytic reactions occurred at high temperatures.

Acknowledgements

Financial support from the Ministry of Science and Technology of China (2001AA 324060) and the Natural Science Foundation of China (20177022) is gratefully acknowledged.

References

[1] J.M. Longo, P.M. Raccah, J. Solid State Chem. 6 (1973) 526.
[2] R.J.H. Voorhoeve, Advanced Materials in Catalysis, Academic Press, New York, 1977, p. 129.
[3] R.J.H. Voorhoeve, D.W. Johnson, J.P. Remeika, P.K. Gallagher, Science 195 (1977) 827.
[4] T. Nitadori, S. Kurihara, M. Misono, J. Catal. 98 (1986) 221.
[5] R.J. Voorhoeve, J.P. Remeika, L.E. Trimble, Ann. NY Acad. Sci. 271 (1976) 3.
[6] V.C. Belessi, C.N. Costa, T.V. Bakas, T. Anastasiadou, P.J. Pomonis, A.M. Efstathiou, Catal. Today 59 (2000) 347.
[7] A.A. Leontiou, A.K. Ladavos, P.J. Pomonis, Appl. Catal. A 241 (2003) 133.
[8] A.A. Leontiou, A.K. Ladavos, G.S. Armatas, P.N. Trikalitis, P.J. Pomonis, Appl. Catal. A 263 (2004) 227.
[9] H. Dai, H. He, P. Li, L. Gao, C.T. Au, Catal. Today 90 (2004) 231.
[10] J. Zhu, D. Xiao, J. Li, X. Yang, Y. Wu, Electrochem. Commun. 7 (2005) 58.
[11] Z.L. Yu, L.Z. Gao, S.Y. Yuan, Y. Wu, J. Chem. Soc., Faraday Trans. 88 (1992) 3245.
[12] Z. Zhao, X. Yang, Y. Wu, Environ. Chem. (Chinese) 14 (1995) 402.
[13] Z. Zhao, X.G. Yang, Y. Wu, Appl. Catal. B 8 (1996) 281.
[14] D.C. Harris, T.A. Hewton, J. Solid State Chem. 69 (1989) 182.
[15] Z. Zhao, Ph.D. Thesis, Changchun Institute of Applied Chemistry, Chinese Academy of Sciences, 1996.
[16] H. Yasuda, N. Mizuno, M. Misono, J. Chem. Soc., Chem. Commun. (1990) 1094.
[17] T. Takahashi, F. Maeda, et al., Phys. Rev. B 36 (1987) 5686.
[18] N. Yamazoe, Y. Teraoka, T. Seiyama, Chem. Lett. (1981) 1767.
[19] F. Patcas, F.C. Buciuman, J. Zsako, Thermochim. Acta 360 (2000) 71.
[20] N. Mizuno, M. Yamato, M. Misono, J. Chem. Soc., Chem. Commun. (1988) 88723.
[21] H. Arai, Hyomen 14 (1976) 427.